
SoftSort: A Continuous Relaxation for the argsort Operator

Sebastian Prillo^{*1} Julian Martin Eisenschlos^{*2}

Abstract

While sorting is an important procedure in computer science, the `argsort` operator - which takes as input a vector and returns its sorting permutation - has a discrete image and thus zero gradients almost everywhere. This prohibits end-to-end, gradient-based learning of models that rely on the `argsort` operator. A natural way to overcome this problem is to replace the `argsort` operator with a continuous relaxation. Recent work has shown a number of ways to do this, but the relaxations proposed so far are computationally complex. In this work we propose a simple continuous relaxation for the `argsort` operator which has the following qualities: it can be implemented in three lines of code, achieves state-of-the-art performance, is easy to reason about mathematically - substantially simplifying proofs - and is faster than competing approaches. We open source the code to reproduce all of the experiments and results.

1. Introduction

Gradient-based optimization lies at the core of the success of deep learning. However, many common operators have discrete images and thus exhibit zero gradients almost everywhere, making them unsuitable for gradient-based optimization. Examples include the *Heaviside step* function, the `argmax` operator, and - the central object of this work - the `argsort` operator. To overcome this limitation, continuous relaxations for these operators can be constructed. For example, the sigmoid function serves as a continuous relaxation for the *Heaviside step* function, and the `softmax` operator serves as a continuous relaxation for the `argmax`. These continuous relaxations have the crucial property that they provide meaningful gradients that can drive optimiza-

^{*}Equal contribution ¹University of California, Berkeley, California, USA ²Google Research, Zurich, Switzerland. Correspondence to: Sebastian Prillo <sprillo@berkeley.edu>, Julian Martin Eisenschlos <eisenjulian@google.com>.

tion. Because of this, operators such as the `softmax` are ubiquitous in deep learning. In this work we are concerned with continuous relaxations for the `argsort` operator.

Formally, we define the `argsort` operator as the mapping $\text{argsort} : \mathbb{R}^n \rightarrow \mathcal{S}_n$ from n -dimensional real vectors $s \in \mathbb{R}^n$ to the set of permutations over n elements $\mathcal{S}_n \subseteq \{1, 2, \dots, n\}^n$, where $\text{argsort}(s)$ returns the permutation that sorts s in decreasing order¹. For example, for the input vector $s = [9, 1, 5, 2]^T$ we have $\text{argsort}(s) = [1, 3, 4, 2]^T$. If we let $\mathcal{P}_n \subseteq \{0, 1\}^{n \times n} \subset \mathbb{R}^{n \times n}$ denote the set of permutation matrices of dimension n , following (Grover et al., 2019) we can define, for a permutation $\pi \in \mathcal{S}_n$, the permutation matrix $P_\pi \in \mathcal{P}_n$ as:

$$P_\pi[i, j] = \begin{cases} 1 & \text{if } j = \pi_i, \\ 0 & \text{otherwise} \end{cases}$$

This is simply the one-hot representation of π . Note that with these definitions, the mapping `sort` : $\mathbb{R}^n \rightarrow \mathbb{R}^n$ that sorts s in decreasing order is $\text{sort}(s) = P_{\text{argsort}(s)}s$. Also, if we let $\bar{\mathbf{1}}_n = [1, 2, \dots, n]^T$, then the `argsort` operator can be recovered from $P_{\text{argsort}(\cdot)} : \mathbb{R}^n \rightarrow \mathcal{P}_n$ by a simple matrix multiplication via

$$\text{argsort}(s) = P_{\text{argsort}(s)}\bar{\mathbf{1}}_n$$

Because of this reduction from the `argsort` operator to the $P_{\text{argsort}(\cdot)}$ operator, in this work, as in previous works (Mena et al., 2018; Grover et al., 2019; Cuturi et al., 2019), our strategy to derive a continuous relaxation for the `argsort` operator is to instead derive a continuous relaxation for the $P_{\text{argsort}(\cdot)}$ operator. This is analogous to the way that the `softmax` operator relaxes the `argmax` operator.

The main contribution of this paper is the proposal of a family of simple continuous relaxation for the $P_{\text{argsort}(\cdot)}$ operator, which we call `SoftSort`, and define as follows:

$$\text{SoftSort}_\tau^d(s) = \text{softmax} \left(\frac{-d(\text{sort}(s)\mathbf{1}^T, \mathbf{1}s^T)}{\tau} \right)$$

where the `softmax` operator is applied row-wise, d is any differentiable almost everywhere, semi-metric function of

¹This is called the `sort` operator in (Grover et al., 2019). We adopt the more conventional naming.

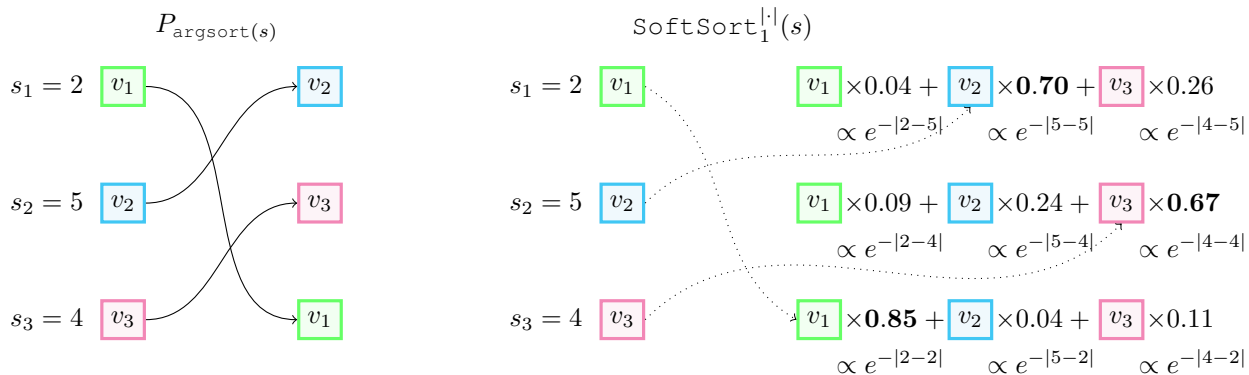


Figure 1. Left: Standard P_{argsort} operation of real value scores s_i on the corresponding vectors v_i . The output is a permutation of the vectors to match the decreasing order of the scores s_i . Right: SoftSort operator applied to the same set of scores and vectors. The output is now a sequence of convex combinations of the vectors that approximates the one on the left and is differentiable with respect to s .

\mathbb{R} applied pointwise, and τ is a temperature parameter that controls the degree of the approximation. In simple words: *the r -th row of the SoftSort operator is the softmax of the negative distances to the r -th largest element.*

Throughout this work we will predominantly use $d(x, y) = |x - y|$ (the L_1 norm), but our theoretical results hold for any such d , making the approach flexible. The SoftSort operator is trivial to implement in automatic differentiation libraries such as TensorFlow (Abadi et al., 2016) and PyTorch (Paszke et al., 2017), and we show that:

- SoftSort achieves state-of-the-art performance on multiple benchmarks that involve reordering elements.
- SoftSort shares the same desirable properties as the NeuralSort operator (Grover et al., 2019). Namely, it is row-stochastic, converges to $P_{\text{argsort}(\cdot)}$ in the limit of the temperature, and can be projected onto a permutation matrix using the row-wise argmax operation. However, SoftSort is significantly easier to reason about mathematically, which substantially simplifies the proof of these properties.
- The SoftSort operator is faster than the NeuralSort operator of (Grover et al., 2019), the fastest competing approach, and empirically just as easy to optimize in terms of the number of gradient steps required for the training objective to converge.

Therefore, the SoftSort operator advances the state of the art in differentiable sorting by significantly simplifying previous approaches. To better illustrate the usefulness of the mapping defined by SoftSort , we show in Figure 1 the result of applying the operator to soft-sort a sequence of vectors v_i ($1 \leq i \leq n$) according to the order given by respective scores $s_i \in \mathbb{R}$. Soft-sorting the v_i is achieved by multiplying to the left by $\text{SoftSort}(s)$.

The code and experiments are available at <https://github.com/sprillo/softsort>

2. Related Work

Relaxed operators for sorting procedures were first proposed in the context of Learning to Rank with the end goal of enabling direct optimization of Information Retrieval (IR) metrics. Many IR metrics, such as the Normalized Discounted Cumulative Gain (NDCG) (Järvelin & Kekäläinen, 2002), are defined in terms of *ranks*. Formally, the rank operator is defined as the function $\text{rank} : \mathbb{R}^n \rightarrow \mathcal{S}_n$ that returns the inverse of the argsort permutation: $\text{rank}(s) = \text{argsort}(s)^{-1}$, or equivalently $P_{\text{rank}(s)} = P_{\text{argsort}(s)}^T$. The rank operator is thus intimately related to the argsort operator; in fact, a relaxation for the $P_{\text{rank}(\cdot)}$ operator can be obtained by transposing a relaxation for the $P_{\text{argsort}(\cdot)}$ operator, and vice-versa; this duality is apparent in the work of (Cuturi et al., 2019).

We begin by discussing previous work on relaxed rank operators in section 2.1. Next, we discuss more recent work, which deals with relaxations for the $P_{\text{argsort}(\cdot)}$ operator.

2.1. Relaxed Rank Operators

The first work to propose a relaxed rank operator is that of (Taylor et al., 2008). The authors introduce the relaxation $\text{SoftRank}_\tau : \mathbb{R}^n \rightarrow \mathbb{R}^n$ given by $\text{SoftRank}_\tau(s) = \mathbb{E}[\text{rank}(s + z)]$ where $z \sim \mathcal{N}_n(0, \tau I_n)$, and show that this relaxation, as well as its gradients, can be computed exactly in time $\mathcal{O}(n^3)$. Note that as $\tau \rightarrow 0$, $\text{SoftRank}_\tau(s) \rightarrow \text{rank}(s)^2$. This relaxation is used in turn to define a surrogate for NDCG which can be optimized directly.

²Except when there are ties, which we assume is not the case. Ties are merely a technical nuisance and do not represent a problem for any of the methods (ours or other’s) discussed in this paper.

In (Qin et al., 2010), another relaxation for the `rank` operator $\widehat{\pi}_\tau : \mathbb{R}^n \rightarrow \mathbb{R}^n$ is proposed, defined as:

$$\widehat{\pi}_\tau(s)[i] = 1 + \sum_{j \neq i} \sigma \left(\frac{s_i - s_j}{\tau} \right) \quad (1)$$

where $\sigma(x) = (1 + \exp\{-x\})^{-1}$ is the sigmoid function. Again, $\widehat{\pi}_\tau(s) \rightarrow \text{rank}(s)$ as $\tau \rightarrow 0$. This operator can be computed in time $\mathcal{O}(n^2)$, which is faster than the $\mathcal{O}(n^3)$ approach of (Taylor et al., 2008).

Note that the above two approaches cannot be used to define a relaxation for the `argsort` operator. Indeed, `SoftRank` $_\tau(s)$ and $\widehat{\pi}_\tau(s)$ are not relaxations for the $P_{\text{rank}(\cdot)}$ operator. Instead, they directly relax the `rank` operator, and there is no easy way to obtain a relaxed `argsort` or $P_{\text{argsort}(\cdot)}$ operator from them.

2.2. Sorting via Bipartite Maximum Matchings

The work of (Mena et al., 2018) draws an analogy between the `argmax` operator and the `argsort` operator by means of bipartite maximum matchings: the `argmax` operator applied to an n -dimensional vector s can be viewed as a maximum matching on a bipartite graph with n vertices in one component and 1 vertex in the other component, the edge weights equal to the given vector s ; similarly, a permutation matrix can be seen as a maximum matching on a bipartite graph between two groups of n vertices with edge weights given by a matrix $X \in \mathbb{R}^{n \times n}$. This induces a mapping M (for ‘matching’) from the set of square matrices $X \in \mathbb{R}^{n \times n}$ to the set \mathcal{P}_n . Note that this mapping has arity $M : \mathbb{R}^{n \times n} \rightarrow \mathcal{P}_n$, unlike the $P_{\text{argsort}(\cdot)}$ operator which has arity $P_{\text{argsort}(\cdot)} : \mathbb{R}^n \rightarrow \mathcal{P}_n$.

Like the $P_{\text{argsort}(\cdot)}$ operator, the M operator has discrete image \mathcal{P}_n , so to enable end-to-end gradient-based optimization, (Mena et al., 2018) propose to relax the matching operator $M(X)$ by means of the Sinkhorn operator $S(X/\tau)$; τ is a temperature parameter that controls the degree of the approximation; as $\tau \rightarrow 0$ they show that $S(X/\tau) \rightarrow M(X)$. The Sinkhorn operator S maps the square matrix X/τ to the Birkhoff polytope \mathcal{B}_n , which is defined as the set of doubly stochastic matrices (i.e. rows and columns summing to 1).

The computational complexity of the (Mena et al., 2018) approach to differentiable sorting is thus $\mathcal{O}(Ln^2)$ where L is the number of Sinkhorn iterates used to approximate $S(X/\tau)$; the authors use $L = 20$ for all experiments.

2.3. Sorting via Optimal Transport

The recent work of (Cuturi et al., 2019) also makes use of the Sinkhorn operator to derive a continuous relaxation for the $P_{\text{argsort}(\cdot)}$ operator. This time, the authors are motivated by the observation that a sorting permutation for $s \in \mathbb{R}^n$ can be recovered from an optimal transport plan between

two discrete measures defined on the real line, one of which is supported on the elements of s and the other of which is supported on arbitrary values $y_1 < \dots < y_n$. Indeed, the optimal transport plan between the probability measures $\frac{1}{n} \sum_{i=1}^n \delta_{s_i}$ and $\frac{1}{n} \sum_{i=1}^n \delta_{y_i}$ (where δ_x is the Dirac delta at x) is given by the matrix $P_{\text{argsort}(s)}^T$.

Notably, a variant of the optimal transport problem with entropy regularization yields instead a continuous relaxation $P_{\text{argsort}(s)}^\epsilon$ mapping s to the Birkhoff polytope \mathcal{B}_n ; ϵ plays a role similar to the temperature in (Mena et al., 2018), with $P_{\text{argsort}(s)}^\epsilon \rightarrow P_{\text{argsort}(s)}$ as $\epsilon \rightarrow 0$. This relaxation can be computed via Sinkhorn iterates, and enables the authors to relax $P_{\text{argsort}(\cdot)}$ by means of $P_{\text{argsort}(s)}^\epsilon$. Gradients can be computed by backpropagating through the Sinkhorn operator as in (Mena et al., 2018).

The computational complexity of this approach is again $\mathcal{O}(Ln^2)$. However, the authors show that a generalization of their method can be used to compute relaxed quantiles in time $\mathcal{O}(Ln)$, which is interesting in its own right.

2.4. Sorting via a sum-of-top-k elements identity

Finally, a more computationally efficient approach to differentiable sorting is proposed in (Grover et al., 2019). The authors rely on an identity that expresses the sum of the top k elements of a vector $s \in \mathbb{R}^n$ as a symmetric function of s_1, \dots, s_n that only involves `max` and `min` operations (Ogryczak & Tamir, 2003, Lemma 1). Based on this identity, and denoting by A_s the matrix of *absolute* pairwise differences of elements of s , namely $A_s[i, j] = |s_i - s_j|$, the authors prove the identity:

$$P_{\text{argsort}(s)}[i, j] = \begin{cases} 1 & \text{if } j = \text{argmax}(c_i), \\ 0 & \text{otherwise} \end{cases} \quad (2)$$

where $c_i = (n + 1 - 2i)s - A_s \mathbf{1}$, and $\mathbf{1}$ denotes the column vector of all ones.

Therefore, by replacing the `argmax` operator in Eq. 2 by a row-wise `softmax`, the authors arrive at the following continuous relaxation for the $P_{\text{argsort}(\cdot)}$ operator, which they call `NeuralSort`:

$$\text{NeuralSort}_\tau(s)[i, :] = \text{softmax} \left(\frac{c_i}{\tau} \right) \quad (3)$$

Again, $\tau > 0$ is a temperature parameter that controls the degree of the approximation; as $\tau \rightarrow 0$ they show that $\text{NeuralSort}_\tau(s) \rightarrow P_{\text{argsort}(s)}$. Notably, the relaxation proposed by (Grover et al., 2019) can be computed in time $\mathcal{O}(n^2)$, making it much faster than the competing approaches of (Mena et al., 2018; Cuturi et al., 2019).

$$\text{NeuralSort}_\tau(s) = g_\tau \begin{pmatrix} 0 & s_2 - s_1 & 3s_3 - s_1 - 2s_2 & 5s_4 - s_1 - 2s_2 - 2s_3 \\ s_2 - s_1 & 0 & s_3 - s_2 & 3s_4 - s_2 - 2s_3 \\ 2s_2 + s_3 - 3s_1 & s_3 - s_2 & 0 & s_4 - s_3 \\ 2s_2 + 2s_3 + s_4 - 5s_1 & 2s_3 + s_4 - 3s_2 & s_4 - s_3 & 0 \end{pmatrix}$$

Figure 2. The 4-dimensional `NeuralSort` operator on the region of space where $s_1 \geq s_2 \geq s_3 \geq s_4$. We define $g_\tau(X)$ as a row-wise softmax with temperature: $\text{softmax}(X/\tau)$. As the most closely related work, this is the main baseline for our experiments.

$$\text{SoftSort}_\tau^{|\cdot|}(s) = g_\tau \begin{pmatrix} 0 & s_2 - s_1 & s_3 - s_1 & s_4 - s_1 \\ s_2 - s_1 & 0 & s_3 - s_2 & s_4 - s_2 \\ s_3 - s_1 & s_3 - s_2 & 0 & s_4 - s_3 \\ s_4 - s_1 & s_4 - s_2 & s_4 - s_3 & 0 \end{pmatrix}$$

Figure 3. The 4-dimensional `SoftSort` operator on the region of space where $s_1 \geq s_2 \geq s_3 \geq s_4$ using $d = |\cdot|$. We define $g_\tau(X)$ as a row-wise softmax with temperature: $\text{softmax}(X/\tau)$. Our formulation is much simpler than previous approaches.

3. SoftSort: A simple relaxed sorting operator

In this paper we propose `SoftSort`, a simple continuous relaxation for the $P_{\text{argsort}(\cdot)}$ operator. We define `SoftSort` as follows:

$$\text{SoftSort}_\tau^d(s) = \text{softmax} \left(\frac{-d(\text{sort}(s)\mathbf{1}^T, \mathbf{1}s^T)}{\tau} \right) \quad (4)$$

where $\tau > 0$ is a temperature parameter that controls the degree of the approximation and d is semi-metric function applied pointwise that is differentiable almost everywhere. Recall that a semi-metric has all the properties of a metric except the triangle inequality, which is not required. Examples of semi-metrics in \mathbb{R} include any positive power of the absolute value. The `SoftSort` operator has similar desirable properties to those of the `NeuralSort` operator, while being significantly simpler. Here we state and prove these properties. We start with the definition of *Unimodal Row Stochastic Matrices* (Grover et al., 2019), which summarizes the properties of our relaxed operator:

Definition 1 (*Unimodal Row Stochastic Matrices*). An $n \times n$ matrix is *Unimodal Row Stochastic (URS)* if it satisfies the following conditions:

1. **Non-negativity:** $U[i, j] \geq 0 \quad \forall i, j \in \{1, 2, \dots, n\}$.
2. **Row Affinity:** $\sum_{j=1}^n U[i, j] = 1 \quad \forall i \in \{1, 2, \dots, n\}$.
3. **Argmax Permutation:** Let u denote a vector of size n such that $u_i = \arg \max_j U[i, j] \quad \forall i \in \{1, 2, \dots, n\}$. Then, $u \in \mathcal{S}_n$, i.e., it is a valid permutation.

While `NeuralSort` and `SoftSort` yield URS matrices (we will prove this shortly), the approaches of (Mena et al.,

2018; Cuturi et al., 2019) yield bistochastic matrices. It is natural to ask whether URS matrices should be preferred over bistochastic matrices for relaxing the $P_{\text{argsort}(\cdot)}$ operator. Note that URS matrices are not comparable to bistochastic matrices: they drop the column-stochasticity condition, but require that each row have a distinct `argmax`, which is not true of bistochastic matrices. This means that URS matrices can be trivially projected onto the probability simplex, which is useful for e.g. straight-through gradient optimization, or whenever hard permutation matrices are required, such as at test time. The one property URS matrices lack is column-stochasticity, but this is not central to soft sorting. Instead, this property arises in the work of (Mena et al., 2018) because their goal is to relax the bipartite matching operator (rather than the `argsort` operator), and in this context bistochastic matrices are the natural choice. Similarly, (Cuturi et al., 2019) yields bistochastic matrices because they are the solutions to optimal transport problems (this does, however, allow them to simultaneously relax the `argsort` and rank operators). Since our only goal (as in the `NeuralSort` paper) is to relax the `argsort` operator, column-stochasticity can be dropped, and URS matrices are the more natural choice.

Now on to the main Theorem, which shows that `SoftSort` has the same desirable properties as `NeuralSort`. These are (Grover et al., 2019, Theorem 4):

Theorem 1 *The SoftSort operator has the following properties:*

1. **Unimodality:** $\forall \tau > 0$, $\text{SoftSort}_\tau^d(s)$ is a unimodal row stochastic matrix. Further, let u denote the permutation obtained by applying `argmax` row-wise to $\text{SoftSort}_\tau^d(s)$. Then, $u = \text{argsort}(s)$.

2. *Limiting behavior: If no elements of s coincide, then:*

$$\lim_{\tau \rightarrow 0^+} \text{SoftSort}_\tau^d(s) = P_{\text{argsort}(s)}$$

In particular, this limit holds almost surely if the entries of s are drawn from a distribution that is absolutely continuous w.r.t. the Lebesgue measure on \mathbb{R} .

Proof.

1. Non-negativity and row affinity follow from the fact that every row in $\text{SoftSort}_\tau^d(s)$ is the result of a `softmax` operation. For the third property, we use that `softmax` preserves maximums and that $d(\cdot, x)$ has a unique minimum at x for every $x \in \mathbb{R}$. Formally, let $\text{sort}(s) = [s_{[1]}, \dots, s_{[n]}]^T$, i.e. $s_{[1]} \geq \dots \geq s_{[n]}$ are the decreasing order statistics of s . Then:

$$\begin{aligned} u_i &= \arg \max_j \text{SoftSort}_\tau^d(s)[i, j] \\ &= \arg \max_j (\text{softmax}(-d(s_{[i]}, s_j)/\tau)) \\ &= \arg \min_j (d(s_{[i]}, s_j)) \\ &= \text{argsort}(s)[i] \end{aligned}$$

as desired.

2. It suffices to show that the i -th row of $\text{SoftSort}_\tau^d(s)$ converges to the one-hot representation h of $\text{argsort}(s)[i]$. But by part 1, the i -th row of $\text{SoftSort}_\tau^d(s)$ is the `softmax` of v/τ where v is a vector whose unique `argmax` is $\text{argsort}(s)[i]$. Since it is a well-known property of the `softmax` that $\lim_{\tau \rightarrow 0^+} \text{softmax}(v/\tau) = h$ (Elfadel & Wyatt, 1994), we are done.

Note that the proof of unimodality of the `SoftSort` operator is straightforward, unlike the proof for the `NeuralSort` operator, which requires proving a more technical Lemma and Corollary (Grover et al., 2019, Lemma 2, Corollary 3).

The row-stochastic property can be loosely interpreted as follows: row r of `SoftSort` and `NeuralSort` encodes a distribution over the value of the rank r element, more precisely, the probability of it being equal to s_j for each j . In particular, note that the first row of the `SoftSort`¹ operator is precisely the `softmax` of the input vector. In general, the r -th row of the `SoftSort` ^{d} operator is the `softmax` of the negative distances to the r -th largest element.

Finally, regarding the choice of d in `SoftSort`, even though a large family of semi-metrics could be considered, in this work we experimented with the absolute value as well as the square distance and found the absolute value to

be marginally better during experimentation. With this in consideration, in what follows we fix $d = |\cdot|$ the absolute value function, unless stated otherwise. We leave for future work learning the metric d or exploring a larger family of such functions.

4. Comparing SoftSort to NeuralSort

4.1. Mathematical Simplicity

The difference between `SoftSort` and `NeuralSort` becomes apparent once we write down what the actual operators look like; the equations defining them (Eq. 3, Eq. 4) are compact but do not offer much insight. Note that even though the work of (Grover et al., 2019) shows that the `NeuralSort` operator has the desirable properties of Theorem 1, the paper never gives a concrete example of what the operator instantiates in practice, which keeps some of its complexity hidden.

Let $g_\tau : \mathbb{R}^{n \times n} \rightarrow \mathbb{R}^{n \times n}$ be the function defined as $g_\tau(X) = \text{softmax}(X/\tau)$, where the `softmax` is applied row-wise. Suppose that $n = 4$ and that s is sorted in decreasing order $s_1 \geq s_2 \geq s_3 \geq s_4$. Then the `NeuralSort` operator is given in Figure 2 and the `SoftSort` operator is given in Figure 3. Note that the diagonal of the logit matrix has been 0-centered by subtracting a constant value from each row; this does not change the `softmax` and simplifies the expressions. The `SoftSort` operator is straightforward, with the i, j -th entry of the logit matrix given by $-|s_i - s_j|$. In contrast, the i, j -th entry of the `NeuralSort` operator depends on all intermediate values s_i, s_{i+1}, \dots, s_j . This is a consequence of the coupling between the `NeuralSort` operator and the complex identity used to derive it. As we show in this paper, this complexity can be completely avoided, and results in further benefits beyond aesthetic simplicity such as flexibility, speed and mathematical simplicity.

Note that for an arbitrary region of space other than $s_1 \geq s_2 \geq s_3 \geq s_4$, the `NeuralSort` and `SoftSort` operators look just like Figures 2 and 3 respectively except for relabelling of the s_i and column permutations. Indeed, we have:

Proposition 1 *For both $f = \text{SoftSort}_\tau^d$ and $f = \text{NeuralSort}_\tau$, the following identity holds:*

$$f(s) = f(\text{sort}(s))P_{\text{argsort}(s)} \quad (5)$$

We defer the proof to appendix B. This proposition is interesting because it implies that the behaviour of the `SoftSort` and `NeuralSort` operators can be completely characterized by their functional form on the region of space where $s_1 \geq s_2 \geq \dots \geq s_n$. Indeed, for any other value of s , we can compute the value of

```

def neural_sort(s, tau):
    n = tf.shape(s)[1]
    one = tf.ones((n, 1), dtype = tf.float32)
    A_s = tf.abs(s - tf.transpose(s, perm=[0, 2, 1]))
    B = tf.matmul(A_s, tf.matmul(one, tf.transpose(one)))
    scaling = tf.cast(n + 1 - 2 * (tf.range(n) + 1), dtype = tf.float32)
    C = tf.matmul(s, tf.expand_dims(scaling, 0))
    P_max = tf.transpose(C-B, perm=[0, 2, 1])
    P_hat = tf.nn.softmax(P_max / tau, -1)
    return P_hat

```

Figure 4. Implementation of NeuralSort in TensorFlow as given in (Grover et al., 2019)

```

def soft_sort(s, tau):
    s_sorted = tf.sort(s, direction='DESCENDING', axis=1)
    pairwise_distances = -tf.abs(tf.transpose(s, perm=[0, 2, 1]) - s_sorted)
    P_hat = tf.nn.softmax(pairwise_distances / tau, -1)
    return P_hat

```

Figure 5. Implementation of SoftSort in TensorFlow as proposed by us, with $d = |\cdot|$.

SoftSort(s) or NeuralSort(s) by first sorting s , then applying SoftSort or NeuralSort, and finally sorting the columns of the resulting matrix with the inverse permutation that sorts s . In particular, to our point, the proposition shows that Figures 2 and 3 are valid for *all* s up to relabeling of the s_i (by $s_{[i]}$) and column permutations (by the inverse permutation that sorts s).

To further our comparison, in appendix D we show how the SoftSort and NeuralSort operators differ in terms of the *size* of their matrix entries.

4.2. Code Simplicity

In Figures 4 and 5 we show TensorFlow implementations of the NeuralSort and SoftSort operators respectively. SoftSort has a simpler implementation than NeuralSort, which we shall see is reflected in its faster speed. (See section 5.5)

Note that our implementation of SoftSort is based directly off Eq. 4, and we rely on the `sort` operator. We would like to remark that there is nothing wrong with using the `sort` operator in a stochastic computation graph. Indeed, the `sort` function is continuous, almost everywhere differentiable (with non-zero gradients) and piecewise linear, just like the `max`, `min` or `ReLU` functions.

Finally, the unimodality property (Theorem 1) implies that any algorithm that builds a relaxed permutation matrix can be used to construct the true discrete permutation matrix. This means that any relaxed sorting algorithm (in particular, NeuralSort) is lower bounded by the complexity of sorting, which justifies relying on sorting as a subroutine. As we show later, SoftSort is faster than NeuralSort. Also, we believe that this modular approach is a net positive

since sorting in CPU and GPU is a well studied problem (Singh et al., 2017) and any underlying improvements will benefit SoftSort’s speed as well. For instance, the current implementation in TensorFlow relies on radix sort and heap sort depending on input size.

5. Experiments

We first compare SoftSort to NeuralSort on the benchmarks from the NeuralSort paper (Grover et al., 2019), using the code kindly open-sourced by the authors. We show that SoftSort performs comparably to NeuralSort. Then, we devise a specific experiment to benchmark the speeds of the SoftSort and NeuralSort operators in isolation, and show that SoftSort is faster than NeuralSort while taking the same number of gradient steps to converge. This makes SoftSort not only the simplest, but also the fastest relaxed sorting operator proposed to date.

5.1. Models

For both SoftSort and NeuralSort we consider their deterministic and stochastic variants as in (Grover et al., 2019). The deterministic operators are those given by equations 3 and 4. The stochastic variants are Plackett-Luce distributions reparameterized via Gumbel distributions (Grover et al., 2019, Section 4.1), where the $P_{\text{argsort}(\cdot)}$ operator that is applied to the samples is relaxed by means of the SoftSort or NeuralSort operator; this is analogous to the Gumbel-Softmax trick where the `argmax` operator that is applied to the samples is relaxed via the `softmax` operator (Jang et al., 2017; Maddison et al., 2017).

SoftSort: A Continuous Relaxation for the `argsort` Operator

ALGORITHM	$n = 3$	$n = 5$	$n = 7$	$n = 9$	$n = 15$
DETERMINISTIC NEURALSORT	0.921 \pm 0.006	0.797 \pm 0.010	0.663 \pm 0.016	0.547 \pm 0.015	0.253 \pm 0.021
STOCHASTIC NEURALSORT	0.918 \pm 0.007	0.801 \pm 0.010	0.665 \pm 0.011	0.540 \pm 0.019	0.250 \pm 0.017
DETERMINISTIC SOFTSORT (OURS)	0.918 \pm 0.005	0.796 \pm 0.009	0.666 \pm 0.016	0.544 \pm 0.015	0.256 \pm 0.023
STOCHASTIC SOFTSORT (OURS)	0.918 \pm 0.005	0.798 \pm 0.005	0.669 \pm 0.018	0.548 \pm 0.019	0.250 \pm 0.020
(CUTURI ET AL., 2019, REPORTED)	0.928	0.811	0.656	0.497	0.126

Table 1. Results for the sorting task averaged over 10 runs. We report the mean and standard deviation for the *proportion of correct permutations*. From $n = 7$ onward, the results are comparable with the state of the art.

ALGORITHM	$n = 5$	$n = 9$	$n = 15$
DETERMINISTIC NEURALSORT	21.52 (0.97)	15.00 (0.97)	18.81 (0.95)
STOCHASTIC NEURALSORT	24.78 (0.97)	17.79 (0.96)	18.10 (0.94)
DETERMINISTIC SOFTSORT (OURS)	23.44 (0.97)	19.26 (0.96)	15.54 (0.95)
STOCHASTIC SOFTSORT (OURS)	26.17 (0.97)	19.06 (0.96)	20.65 (0.94)

Table 2. Results for the quantile regression task. The first metric is the mean squared error ($\times 10^{-4}$) when predicting the median number. The second metric - in parenthesis - is Spearman’s R^2 for the predictions. Results are again comparable with the state of the art.

5.2. Sorting Handwritten Numbers

The *large-MNIST* dataset of handwritten *numbers* is formed by concatenating 4 randomly selected MNIST *digits*. In this task, a neural network is presented with a sequence of n large-MNIST numbers and must learn the permutation that sorts these numbers. Supervision is provided only in the form of the ground-truth permutation. Performance on the task is measured by:

1. The proportion of *permutations* that are perfectly recovered.
2. The proportion of *permutation elements* that are correctly recovered.

Note that the first metric is always less than or equal to the second metric. We use the setup in (Cuturi et al., 2019) to be able to compare against their Optimal-Transport-based method. They use 100 epochs to train all models.

The results for the first metric are shown in Table 5. We report the mean and standard deviation over 10 runs. We see that SoftSort and NeuralSort perform identically for all values of n . Moreover, our results for NeuralSort are better than those reported in (Cuturi et al., 2019), to the extent that NeuralSort and SoftSort outperform the method of (Cuturi et al., 2019) for $n = 9, 15$, unlike reported in said paper. We found that the hyperparameter values reported in (Grover et al., 2019) and used by (Cuturi et al., 2019) for NeuralSort are far from ideal: (Grover et al., 2019) reports using a learning rate of 10^{-4} and temperature values from the set $\{1, 2, 4, 8, 16\}$. However, a higher learning rate dramatically improves NeuralSort’s results, and higher temperatures also help. Concretely, we used a learn-

ing rate of 0.005 for all the SoftSort and NeuralSort models, and a value of $\tau = 1024$ for $n = 3, 5, 7$ and $\tau = 128$ for $n = 9, 15$. The results for the second metric are reported in appendix E. In the appendix we also include learning curves for SoftSort and NeuralSort, which show that they converge at the same speed.

5.3. Quantile Regression

As in the sorting task, a neural network is presented with a sequence of n large-MNIST numbers. The task is to predict the median element from the sequence, and this is the only available form of supervision. Performance on the task is measured by mean squared error and Spearman’s rank correlation. We used 100 iterations to train all models.

The results are shown in Table 5. We used a learning rate of 10^{-3} for all models - again, higher than that reported in (Grover et al., 2019) - and grid-searched the temperature on the set $\{128, 256, 512, 1024, 2048, 4096\}$ - again, higher than that reported in (Grover et al., 2019). We see that SoftSort and NeuralSort perform similarly, with NeuralSort sometimes outperforming SoftSort and vice versa. The results for NeuralSort are also much better than those reported in (Grover et al., 2019), which we attribute to the better choice of hyperparameters, concretely, the higher learning rate. In the appendix we also include learning curves for SoftSort and NeuralSort, which show that they converge at the same speed.

5.4. Differentiable kNN

In this setup, we explored using the SoftSort operator to learn a differentiable k -nearest neighbours (kNN) classifier that is able to learn a representation function, used to

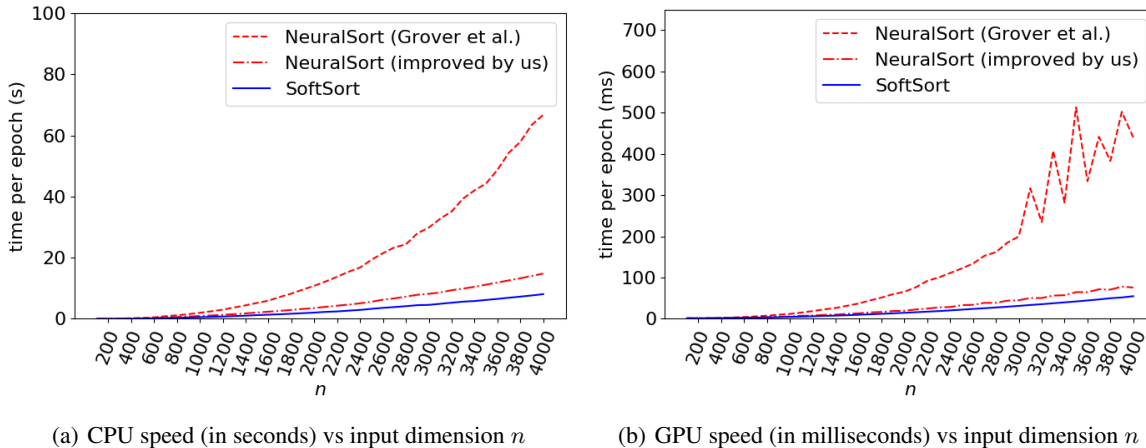


Figure 6. Speed of the NeuralSort and SoftSort operators on (a) CPU and (b) GPU, as a function of n (the size of the vector to be sorted). Twenty vectors of size n are batched together during each epoch. The original NeuralSort implementation is up to 6 times slower on both CPU and GPU. After some performance improvements, NeuralSort is 80% slower on CPU and 40% slower on GPU.

ALGORITHM	MNIST	FASHION-MNIST	CIFAR-10
KNN+PIXELS	97.2%	85.8%	35.4%
KNN+PCA	97.6%	85.9%	40.9%
KNN+AE	97.6%	87.5%	44.2%
KNN + DETERMINISTIC NEURALSORT	99.5%	93.5%	90.7%
KNN + STOCHASTIC NEURALSORT	99.4%	93.4%	89.5%
KNN + DETERMINISTIC SOFTSORT (OURS)	99.37%	93.60%	92.03%
KNN + STOCHASTIC SOFTSORT (OURS)	99.42%	93.67%	90.64%
CNN (W/O KNN)	99.4%	93.4%	95.1%

Table 3. Average test classification accuracy comparing k-nearest neighbor models. The last row includes the results from non kNN classifier. The results are comparable with the state of the art, or above it by a small margin.

measure the distance between the candidates.

In a supervised training framework, we have a dataset that consists of pairs (x, y) of a datapoint and a label. We are interested in learning a map Φ to embed every x such that we can use a kNN classifier to identify the class of \hat{x} by looking at the class of its closest neighbours according to the distance $\|\Phi(x) - \Phi(\hat{x})\|$. Such a classifier would be valuable by virtue of being interpretable and robust to both noise and unseen classes.

This is achieved by constructing episodes during training that consist of one pair \hat{x}, \hat{y} and n candidate pairs (x_i, y_i) for $i = 1 \dots n$, arranged in two column vectors X and Y . The probability $P(\hat{y}|\hat{x}, X, Y)$ of class \hat{y} under a kNN classifier is the average of the first k entries in the vector

$$P_{\text{argsort}}(-\|\Phi(X) - \Phi(\hat{x})\|^2) \mathbb{1}_{Y=\hat{y}}$$

where $\|\Phi(X) - \Phi(\hat{x})\|^2$ is the vector of squared distances from the candidate points and $\mathbb{1}_{Y=\hat{y}}$ is the binary vector indicating which indexes have class \hat{y} . Thus, if we replace

P_{argsort} by the SoftSort operator we obtain a differentiable relaxation $\hat{P}(\hat{y}|\hat{x}, X, Y)$. To compute the loss we follow (Grover et al., 2019) and use $-\hat{P}(\hat{y}|\hat{x}, X, Y)$. We also experimented with the cross entropy loss, but the performance went down for both methods.

When $k = 1$, our method is closely related to *Matching Networks* (Vinyals et al., 2016). This follows from the following result: (See proof in Appendix C)

Proposition 2 *Let $k = 1$ and \hat{P} be the differentiable kNN operator using $\text{SoftSort}_2^{|\cdot|}$. If we choose the embedding function Φ to be of norm 1, then*

$$\hat{P}(\hat{y}|\hat{x}, X, Y) = \sum_{i: y_i=\hat{y}} e^{\Phi(\hat{x}) \cdot \Phi(x_i)} / \sum_{i=1 \dots n} e^{\Phi(\hat{x}) \cdot \Phi(x_i)}$$

This suggests that our method is a generalization of *Matching Networks*, since in our experiments larger values of k yielded better results consistently and we expect a kNN classifier to be more robust in a setup with noisy labels.

However, *Matching Networks* use contextual embedding functions, and different networks for \hat{x} and the candidates x_i , both of which could be incorporated to our setup. A more comprehensive study comparing both methods on a few shot classification dataset such as *Omniglot* (Lake et al., 2011) is left for future work.

We applied this method to three benchmark datasets: MNIST, Fashion MNIST and CIFAR-10 with canonical splits. As baselines, we compare against `NeuralSort` as well as other kNN models with fixed representations coming from raw pixels, a PCA feature extractor and an auto-encoder. All the results are based on the ones reported in (Grover et al., 2019). We also included for comparison a standard classifier using a convolutional network.

Results are shown in Table 5. In every case, we achieve comparable accuracies with `NeuralSort` implementation, either slightly outperforming or underperforming `NeuralSort`. See hyperparameters used in appendix A.

5.5. Speed Comparison

We set up an experiment to compare the speed of the `SoftSort` and `NeuralSort` operators. We are interested in exercising both their forward and backward calls. To this end, we set up a dummy learning task where the goal is to perturb an n -dimensional input vector θ to make it become sorted. We scale θ to $[0, 1]$ and feed it through the `SoftSort` or `NeuralSort` operator to obtain $\hat{P}(\theta)$, and place a loss on $\hat{P}(\theta)$ that encourages it to become equal to the identity matrix, and thus encourages the input to become sorted.

Concretely, we place the cross-entropy loss between the true permutation matrix and the predicted soft URS matrix:

$$L(\hat{P}) = -\frac{1}{n} \sum_{i=1}^n \log \hat{P}[i, i]$$

This encourages the probability mass from each row of \hat{P} to concentrate on the diagonal, which drives θ to sort itself. Note that this is a trivial task, since for example a pointwise ranking loss $\frac{1}{n} \sum_{i=1}^n (\theta_i + i)^2$ (Taylor et al., 2008, Section 2.2) leads the input to become sorted too, without any need for the `SoftSort` or `NeuralSort` operators. However, this task is a reasonable benchmark to measure the speed of the two operators in a realistic learning setting.

We benchmark n in the range 100 to 4000, and batch 20 inputs θ together to exercise batching. Thus the input is a parameter tensor of shape $20 \times n$. Models are trained for 100 epochs, which we verified is enough for the parameter vectors to become perfectly sorted by the end of training (i.e., to succeed at the task).

In Figure 6 we show the results for the TensorFlow im-

plementations of `NeuralSort` and `SoftSort` given in Figures 4 and 5 respectively. We see that on both CPU and GPU, `SoftSort` is faster than `NeuralSort`. For $N = 4000$, `SoftSort` is about 6 times faster than the `NeuralSort` implementation of (Grover et al., 2019) on both CPU and GPU. We tried to speed up the `NeuralSort` implementation of (Grover et al., 2019), and although we were able to improve it, `NeuralSort` was still slower than `SoftSort`, concretely: 80% slower on CPU and 40% slower on GPU. Details of our improvements to the speed of the `NeuralSort` operator are provided in appendix A.4.5.

The performance results for PyTorch are provided in the appendix and are similar to the TensorFlow results. In the appendix we also show that the learning curves of `SoftSort` with $d = |\cdot|^2$ and `NeuralSort` are almost identical; interestingly, we found that using $d = |\cdot|$ converges more slowly on this synthetic task.

We also investigated if relying on a sorting routine could cause slower run times in worst-case scenarios. When using sequences sorted in the opposite order we did not note any significant slowdowns. Furthermore, in applications where this could be a concern, the effect can be avoided entirely by shuffling the inputs before applying our operator.

As a final note, given that the cost of sorting is sub-quadratic, and most of the computation is payed when building and applying the $n \times n$ matrix, we also think that our algorithm could be made faster asymptotically by constructing sparse versions of the `SoftSort` operator. For applications like differentiable nearest neighbors, evidence suggests than processing longer sequences yields better results, which motivates improvements in the asymptotic complexity. We leave this topic for future work.

6. Conclusion

We have introduced `SoftSort`, a simple continuous relaxation for the `argsort` operator. The r -th row of the `SoftSort` operator is simply the softmax of the negative distances to the r -th largest element.

`SoftSort` has similar properties to those of the `NeuralSort` operator of (Grover et al., 2019). However, due to its simplicity, `SoftSort` is trivial to implement, more modular, faster than `NeuralSort`, and proofs regarding the `SoftSort` operator are effortless. We also empirically find that it is just as easy to optimize.

Fundamentally, `SoftSort` advances the state of the art in differentiable sorting by significantly simplifying previous approaches. Our code and experiments can be found at <https://github.com/sprillo/softsort>.

Acknowledgments

We thank Assistant Professor Jordan Boyd-Graber from University of Maryland and Visting Researcher at Google, and Thomas Miller from Google Language Research at Zurich for their feedback and comments on earlier versions of the manuscript. We would also like to thank the anonymous reviewers for their feedback that helped improve this work.

References

- Abadi, M., Barham, P., Chen, J., Chen, Z., Davis, A., Dean, J., Devin, M., Ghemawat, S., Irving, G., Isard, M., Kudlur, M., Levenberg, J., Monga, R., Moore, S., Murray, D. G., Steiner, B., Tucker, P., Vasudevan, V., Warden, P., Wicke, M., Yu, Y., and Zheng, X. Tensorflow: A system for large-scale machine learning. In *12th USENIX Symposium on Operating Systems Design and Implementation (OSDI 16)*, pp. 265–283, 2016.
- Cuturi, M., Teboul, O., and Vert, J.-P. Differentiable ranking and sorting using optimal transport. In Wallach, H., Larochelle, H., Beygelzimer, A., d'Alché-Buc, F., Fox, E., and Garnett, R. (eds.), *Advances in Neural Information Processing Systems 32*, pp. 6858–6868. Curran Associates, Inc., 2019.
- Elfadeli, I. M. and Wyatt, Jr., J. L. The "softmax" nonlinearity: Derivation using statistical mechanics and useful properties as a multiterminal analog circuit element. In Cowan, J. D., Tesauero, G., and Alspector, J. (eds.), *Advances in Neural Information Processing Systems 6*, pp. 882–887. Morgan-Kaufmann, 1994.
- Grover, A., Wang, E., Zweig, A., and Ermon, S. Stochastic optimization of sorting networks via continuous relaxations. In *International Conference on Learning Representations*, 2019.
- He, K., Zhang, X., Ren, S., and Sun, J. Identity mappings in deep residual networks. In Leibe, B., Matas, J., Sebe, N., and Welling, M. (eds.), *Computer Vision – ECCV 2016*, pp. 630–645, Cham, 2016. Springer International Publishing. ISBN 978-3-319-46493-0.
- Jang, E., Gu, S., and Poole, B. Categorical reparameterization with gumbel-softmax. In *International Conference on Learning Representations*, 2017.
- Järvelin, K. and Kekäläinen, J. Cumulated gain-based evaluation of ir techniques. *ACM Trans. Inf. Syst.*, 20(4): 422446, October 2002.
- Lake, B. M., Salakhutdinov, R., Gross, J., and Tenenbaum, J. B. One shot learning of simple visual concepts. In *CogSci*, 2011.
- Maddison, C., Mnih, A., and Teh, Y. The concrete distribution: A continuous relaxation of discrete random variables. In *International Conference on Learning Representations*, 04 2017.
- Mena, G., Belanger, D., Linderman, S., and Snoek, J. Learning latent permutations with gumbel-sinkhorn networks. In *International Conference on Learning Representations*, 2018.
- Ogryczak, W. and Tamir, A. Minimizing the sum of the k largest functions in linear time. *Information Processing Letters*, 85(3):117 – 122, 2003.
- Paszke, A., Gross, S., Chintala, S., Chanan, G., Yang, E., Devito, Z., Lin, Z., Desmaison, A., Antiga, L., and Lerer, A. Automatic differentiation in pytorch. In *Advances in Neural Information Processing Systems 30*, 2017.
- Qin, T., Liu, T.-Y., and Li, H. A general approximation framework for direct optimization of information retrieval measures. *Inf. Retr.*, 13(4):375397, August 2010.
- Singh, D., Joshi, I., and Choudhary, J. Survey of gpu based sorting algorithms. *International Journal of Parallel Programming*, 46, 04 2017. doi: 10.1007/s10766-017-0502-5.
- Taylor, M., Guiver, J., Robertson, S., and Minka, T. Soft-rank: Optimizing non-smooth rank metrics. In *Proceedings of the 2008 International Conference on Web Search and Data Mining, WSDM 08*, pp. 7786, New York, NY, USA, 2008. Association for Computing Machinery. ISBN 9781595939272.
- Vinyals, O., Blundell, C., Lillicrap, T. P., Kavukcuoglu, K., and Wierstra, D. Matching networks for one shot learning. In *Advances in Neural Information Processing Systems 29*, 2016.

A. Experimental Details

We use the code kindly open sourced by (Grover et al., 2019) to perform the sorting, quantile regression, and kNN experiments. As such, we are using the same setup as in (Grover et al., 2019). The work of (Cuturi et al., 2019) also uses this code for the sorting task, allowing for a fair comparison.

To make our work self-contained, in this section we recall the main experimental details from (Grover et al., 2019), and we also provide our hyperparameter settings, which crucially differ from those used in (Grover et al., 2019) by the use of higher learning rates and temperatures (leading to improved results).

A.1. Sorting Handwritten Numbers

A.1.1. ARCHITECTURE

The convolutional neural network architecture used to map 112×28 large-MNIST images to scores is as follows:

```

Conv[Kernel: 5x5, Stride: 1, Output: 112x28x32,
     Activation: Relu]
→Pool[Stride: 2, Output: 56x14x32]
→Conv[Kernel: 5x5, Stride: 1, Output: 56x14x64,
     Activation: Relu]
→Pool[Stride: 2, Output: 28x7x64]
→FC[Units: 64, Activation: Relu]
→FC[Units: 1, Activation: None]

```

Recall that the large-MNIST dataset is formed by concatenating four 28×28 MNIST images, hence each large-MNIST image input is of size 112×28 .

For a given input sequence x of large-MNIST images, using the above CNN we obtain a vector s of scores (one score per image). Feeding this score vector into `NeuralSort` or `SoftSort` yields the matrix $\hat{P}(s)$ which is a relaxation for $P_{\text{argsort}(s)}$.

A.1.2. LOSS FUNCTIONS

To learn to sort the input sequence x of large-MNIST digits, (Grover et al., 2019) imposes a cross-entropy loss between the rows of the true permutation matrix P and the learnt relaxation $\hat{P}(s)$, namely:

$$L = \frac{1}{n} \sum_{i,j=1}^n \mathbb{1}\{P[i,j] = 1\} \log \hat{P}(s)[i,j]$$

This is the loss for one example (x, P) in the deterministic setup. For the stochastic setup with reparameterized

Plackett-Luce distributions, the loss is instead:

$$L = \frac{1}{n} \sum_{i,j=1}^n \sum_{k=1}^{n_s} \mathbb{1}\{P[i,j] = 1\} \log \hat{P}(s + z_k)[i,j]$$

where z_k ($1 \leq k \leq n_s$) are samples from the Gumbel distribution.

A.1.3. HYPERPARAMETERS

For this task we used an Adam optimizer with an initial learning rate of 0.005 and a batch size of 20. The temperature τ was selected from the set $\{1, 16, 128, 1024\}$ based on validation set accuracy on predicting entire permutations. As a results, we used a value of $\tau = 1024$ for $n = 3, 5, 7$ and $\tau = 128$ for $n = 9, 15$. 100 iterations were used to train all models. For the stochastic setting, $n_s = 5$ samples were used.

A.1.4. LEARNING CURVES

In Figure 7 (a) we show the learning curves for deterministic `SoftSort` and `NeuralSort`, with $N = 15$. These are the average learning curves over all 10 runs. Both learning curves are almost identical, showing that in this task both operators can essentially be exchanged for one another.

A.2. Quantile Regression

A.2.1. ARCHITECTURE

The same convolutional neural network as in the sorting task was used to map large-MNIST images to scores. A second neural network g_θ with the same architecture but different parameters is used to regress each image to its value. These two networks are then used by the loss functions below to learn the median element.

A.2.2. LOSS FUNCTIONS

To learn the median element of the input sequence x of large-MNIST digits, (Grover et al., 2019) first soft-sorts x via $\hat{P}(s)x$ which allows extracting the candidate median image. This candidate median image is then mapped to its predicted value \hat{y} via the CNN g_θ . The square loss between \hat{y} and the true median value y is incurred. As in (Grover et al., 2019, Section E.2), the loss for a single example (x, y) can thus compactly be written as (in the deterministic case):

$$L = \|y - g_\theta(\hat{P}(s)x)\|_2^2$$

For the stochastic case, the loss for a single example (x, y) is instead:

$$L = \sum_{k=1}^{n_s} \|y - g_\theta(\hat{P}(s + z_k)x)\|_2^2$$

where z_k ($1 \leq k \leq n_s$) are samples from the Gumbel distribution.

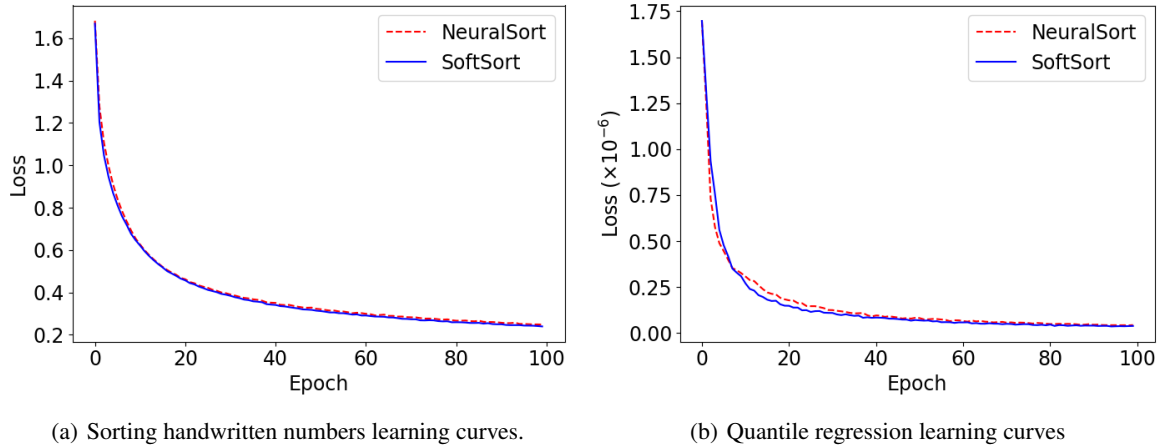


Figure 7. Learning curves for the ‘sorting handwritten numbers’ and ‘quantile regression’ tasks. The learning curves for SoftSort and NeuralSort are almost identical.

Table 4. Values of τ used for the quantile regression task.

ALGORITHM	$n = 5$	$n = 9$	$n = 15$
DETERMINISTIC NEURALSORT	1024	512	1024
STOCHASTIC NEURALSORT	2048	512	4096
DETERMINISTIC SOFTSORT	2048	2048	256
STOCHASTIC SOFTSORT	4096	2048	2048

A.2.3. HYPERPARAMETERS

We used an Adam optimizer with an initial learning rate of 0.001 and a batch size of 5. The value of τ was grid searched on the set $\{128, 256, 512, 1024, 2048, 4096\}$ based on validation set MSE. The final values of τ used to train the models and evaluate test set performance are given in Table 4. 100 iterations were used to train all models. For the stochastic setting, $n_s = 5$ samples were used.

A.2.4. LEARNING CURVES

In Figure 7 (b) we show the learning curves for deterministic SoftSort and NeuralSort, with $N = 15$. Both learning curves are almost identical, showing that in this task both operators can essentially be exchanged for one another.

A.3. Differentiable KNN

A.3.1. ARCHITECTURES

To embed the images before applying differentiable kNN, we used the following convolutional network architectures.

For MNIST:

Conv[Kernel: 5x5, Stride: 1, Output: 24x24x20,
 Activation: Relu]
 →Pool[Stride: 2, Output: 12x12x20]
 →Conv[Kernel: 5x5, Stride: 1, Output: 8x8x50,
 Activation: Relu]
 →Pool[Stride: 2, Output: 4x4x50]
 →FC[Units: 50, Activation: Relu]

and for Fashion-MNIST and CIFAR-10 we used the ResNet18 architecture (He et al., 2016) as defined in github.com/kuangliu/pytorch-cifar, but we keep the 512 dimensional output before the last classification layer.

For the baseline experiments in pixel distance with PCA and kNN, we report the results of (Grover et al., 2019), using *scikit-learn* implementations.

In the auto-encoder baselines, the embeddings were trained using the follow architectures. For MNIST and Fashion-MNIST:

Encoder:
 FC[Units: 500, Activation: Relu]
 →FC[Units: 500, Activation: Relu]
 →FC[Units: 50, Activation: Relu]
 Decoder:
 →FC[Units: 500, Activation: Relu]
 →FC[Units: 500, Activation: Relu]
 →FC[Units: 784, Activation: Sigmoid]

For CIFAR-10, we follow the architecture defined at

github.com/shibuiwilliam/Keras_Autoencoder, with a bottleneck dimension of 256.

A.3.2. LOSS FUNCTIONS

For the models using `SoftSort` or `NeuralSort` we use the negative of the probability output from the kNN model as a loss function. For the auto-encoder baselines we use a per-pixel binary cross entropy loss.

A.3.3. HYPERPARAMETERS

We perform a grid search for $k \in (1, 3, 5, 9)$, $\tau \in (1, 4, 16, 64, 128, 512)$, learning rates taking values in 10^{-3} , 10^{-4} and 10^{-5} . We train for 200 epochs and choose the model based on validation loss. The optimizer used is *SGD* with momentum of 0.9. Every batch has 100 episode, each containing 100 candidates.

A.4. Speed Comparison

A.4.1. ARCHITECTURE

The input parameter vector θ of shape $20 \times n$ (20 being the batch size) is first normalized to $[0, 1]$ and then fed through the `NeuralSort` or `SoftSort` operator, producing an output tensor \hat{P} of shape $20 \times n \times n$.

A.4.2. LOSS FUNCTION

We impose the following loss term over the batch:

$$L(\hat{P}) = -\frac{1}{20} \sum_{i=1}^{20} \frac{1}{n} \sum_{j=1}^n \log \hat{P}[i, j, j]$$

This loss term encourages the probability mass from each row of $\hat{P}[i, :, :]$ to concentrate on the diagonal, i.e. encourages each row of θ to become sorted in decreasing order. We also add an L_2 penalty term $\frac{1}{200} \|\theta\|_2^2$ which ensures that the entries of θ do not diverge during training.

A.4.3. HYPERPARAMETERS

We used 100 epochs to train the models, with the first epoch used as burn-in to warm up the CPU or GPU (i.e. the first epoch is excluded from the time measurement). We used a temperature of $\tau = 100.0$ for `NeuralSort` and $\tau = 0.03$, $d = |\cdot|^2$ for `SoftSort`. The entries of θ are initialized uniformly at random in $[-1, 1]$. A momentum optimizer with learning rate 10 and momentum 0.5 was used. With these settings, 100 epochs are enough to sort each row of θ in decreasing order perfectly for $n = 4000$.

Note that since the goal is to benchmark the operator’s speeds, performance on the Spearman rank correlation metric is anecdotal. However, we took the trouble of tuning the hyperparameters and the optimizer to make the learning

setting as realistic as possible, and to ensure that the entries in θ are not diverging (which would negatively impact and confound the performance results). Finally, note that the learning problem is trivial, as a pointwise loss such as $\sum_{i=1}^{20} \sum_{j=1}^n (\theta_{ij} + j)^2$ sorts the rows of θ without need for the `NeuralSort` or `SoftSort` operator. However, this bare-bones task exposes the computational performance of the `NeuralSort` and `SoftSort` operators.

A.4.4. LEARNING CURVES

In Figure 8 we show the learning curves for $N = 4000$; the Spearman correlation metric is plotted against epoch. We see that `SoftSort` with $d = |\cdot|^2$ and `NeuralSort` have almost identical learning curves. Interestingly, `SoftSort` with $d = |\cdot|$ converges more slowly.

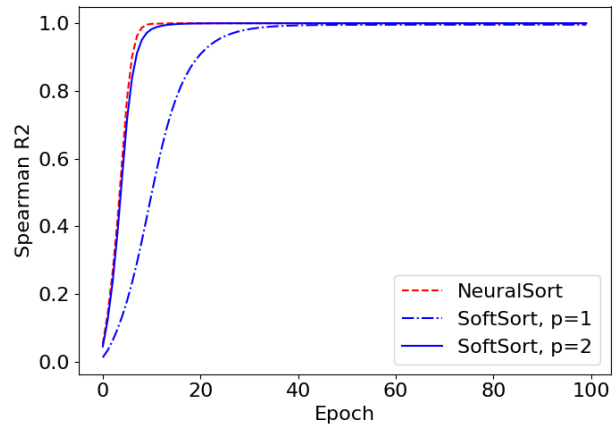


Figure 8. Learning curves for `SoftSort` with $d = |\cdot|^p$ for $p \in \{1, 2\}$, and `NeuralSort`, on the speed comparison task.

A.4.5. NEURALSORT PERFORMANCE IMPROVEMENT

We found that the `NeuralSort` implementations provided by (Grover et al., 2019) in both TensorFlow and PyTorch have complexity $\mathcal{O}(n^3)$. Indeed, in their TensorFlow implementation (Figure 4), the complexity of the following line is $\mathcal{O}(n^3)$:

```
B = tf.matmul(A_s, tf.matmul(one,
                             tf.transpose(one)))
```

since the three matrices multiplied have sizes $n \times n$, $n \times 1$, and $1 \times n$ respectively. To obtain $\mathcal{O}(n^2)$ complexity we associate differently:

```
B = tf.matmul(tf.matmul(A_s, one),
              tf.transpose(one))
```

The same is true for their PyTorch implementation (Fig-

ure 11). This way, we were able to speed up the implementations provided by (Grover et al., 2019).

A.4.6. PYTORCH RESULTS

In Figure 9 we show the benchmarking results for the PyTorch framework (Paszke et al., 2017). These are analogous to the results presented in Figure 6) of the main text. The results are similar to those for the TensorFlow framework, except that for PyTorch, `NeuralSort` runs out of memory on CPU for $n = 3600$, on GPU for $n = 3900$, and `SoftSort` runs out of memory on CPU for $n = 3700$.

A.4.7. HARDWARE SPECIFICATION

We used a GPU V100 and an n1-highmem-2 (2 vCPUs, 13 GB memory) Google Cloud instance to perform the speed comparison experiment.

We were also able to closely reproduce the GPU results on an Amazon EC2 p2.xlarge instance (4 vCPUs, 61 GB memory) equipped with a GPU Tesla K80, and the CPU results on an Amazon EC2 c5.2xlarge instance (8 vCPUs, 16 GB memory).

B. Proof of Proposition 1

First we recall the Proposition:

Proposition. For both $f = \text{SoftSort}_\tau^d$ (with any d) and $f = \text{NeuralSort}_\tau$, the following identity holds:

$$f(s) = f(\text{sort}(s))P_{\text{argsort}(s)} \quad (6)$$

To prove the proposition, we will use the following two Lemmas:

Lemma 1 Let $P \in \mathbb{R}^{n \times n}$ be a permutation matrix, and let $g : \mathbb{R}^k \rightarrow \mathbb{R}$ be any function. Let $G : \underbrace{\mathbb{R}^{n \times n} \times \dots \times \mathbb{R}^{n \times n}}_{k \text{ times}} \rightarrow \mathbb{R}^{n \times n}$ be the pointwise application of g , that is:

$$G(A_1, \dots, A_k)_{i,j} = g((A_1)_{i,j}, \dots, (A_k)_{i,j}) \quad (7)$$

Then the following identity holds for any $A_1, \dots, A_k \in \mathbb{R}^{n \times n}$:

$$G(A_1, \dots, A_k)P = G(A_1P, \dots, A_kP) \quad (8)$$

Proof of Lemma 1. Since P is a permutation matrix, multiplication to the right by P permutes columns according to some permutation, i.e.

$$(AP)_{i,j} = A_{i,\pi(j)} \quad (9)$$

for some permutation π and any $A \in \mathbb{R}^{n \times n}$. Thus, for any fixed i, j :

$$\begin{aligned} & (G(A_1, \dots, A_k)P)_{i,j} \\ & \stackrel{(i)}{=} G(A_1, \dots, A_k)_{i,\pi(j)} \\ & \stackrel{(ii)}{=} g((A_1)_{i,\pi(j)}, \dots, (A_k)_{i,\pi(j)}) \\ & \stackrel{(iii)}{=} g((A_1P)_{i,j}, \dots, (A_kP)_{i,j}) \\ & \stackrel{(iv)}{=} G(A_1P, \dots, A_kP)_{i,j} \end{aligned}$$

where (i), (iii) follow from Eq. 9, and (ii), (iv) follow from Eq. 7. This proves the Lemma. ■

Lemma 2 Let $P \in \mathbb{R}^{n \times n}$ be a permutation matrix, and $\sigma = \text{softmax}$ denote the row-wise softmax, i.e.:

$$\sigma(A)_{i,j} = \frac{\exp\{A_{i,j}\}}{\sum_k \exp\{A_{i,k}\}} \quad (10)$$

Then the following identity holds for any $A \in \mathbb{R}^{n \times n}$:

$$\sigma(A)P = \sigma(AP) \quad (11)$$

Proof of Lemma 2. As before, there exists a permutation π such that:

$$(BP)_{i,j} = B_{i,\pi(j)} \quad (12)$$

for any $B \in \mathbb{R}^{n \times n}$. Thus for any fixed i, j :

$$\begin{aligned} & (\sigma(A)P)_{i,j} \\ & \stackrel{(i)}{=} \sigma(A)_{i,\pi(j)} \\ & \stackrel{(ii)}{=} \frac{\exp\{A_{i,\pi(j)}\}}{\sum_k \exp\{A_{i,\pi(k)}\}} \\ & \stackrel{(iii)}{=} \frac{\exp\{(AP)_{i,j}\}}{\sum_k \exp\{(AP)_{i,k}\}} \\ & \stackrel{(iv)}{=} \sigma(AP)_{i,j} \end{aligned}$$

where (i), (iii) follow from Eq. 12 and (ii), (iv) follow from the definition of the row-wise softmax (Eq. 10). This proves the Lemma. ■

We now leverage the Lemmas to provide proofs of Proposition 1 for each operator. To unclutter equations, we will denote by $\sigma = \text{softmax}$ the row-wise softmax operator.

Proof of Proposition 1 for SoftSort. We have that:

$$\begin{aligned} & \text{SoftSort}_\tau^d(\text{sort}(s))P_{\text{argsort}(s)} \\ & \stackrel{(i)}{=} \sigma\left(\frac{-d(\text{sort}(\text{sort}(s))\mathbf{1}^T, \mathbf{1}_{\text{sort}(s)}^T)}{\tau}\right)P_{\text{argsort}(s)} \\ & \stackrel{(ii)}{=} \sigma\left(\frac{-d(\text{sort}(s)\mathbf{1}^T, \mathbf{1}_{\text{sort}(s)}^T)}{\tau}\right)P_{\text{argsort}(s)} \end{aligned}$$

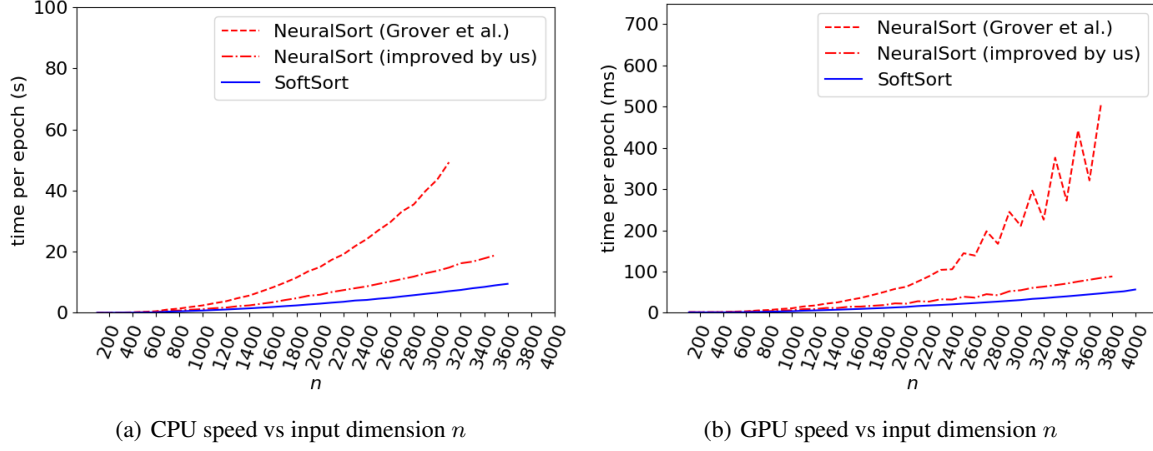


Figure 9. Speed of the NeuralSort and SoftSort operators on (a) CPU and (b) GPU, as a function of n (the size of the vector to be sorted). Twenty vectors of size n are batched together during each epoch. Note that CPU plot y-axis is in seconds (s), while GPU plot y-axis is in milliseconds (ms). Implementation in PyTorch.

where (i) follows from the definition of the SoftSort operator (Eq. 4) and (ii) follows from the idempotence of the sort operator, i.e. $\text{sort}(\text{sort}(s)) = \text{sort}(s)$. Invoking Lemma 2, we can push $P_{\text{argsort}(s)}$ into the softmax:

$$= \sigma\left(\frac{-d(\text{sort}(s)\mathbf{1}^T, \mathbf{1}\text{sort}(s)^T)}{\tau} P_{\text{argsort}(s)}\right)$$

Using Lemma 1 we can further push $P_{\text{argsort}(s)}$ into the pointwise d function:

$$= \sigma\left(\frac{-d(\text{sort}(s)\mathbf{1}^T P_{\text{argsort}(s)}, \mathbf{1}\text{sort}(s)^T P_{\text{argsort}(s)})}{\tau}\right)$$

Now note that $\mathbf{1}^T P_{\text{argsort}(s)} = \mathbf{1}^T$ since P is a permutation matrix and thus the columns of P add up to 1. Also, since $\text{sort}(s)^T = P_{\text{argsort}(s)} s^T$ then $\text{sort}(s)^T P_{\text{argsort}(s)} = s^T P_{\text{argsort}(s)}^T P_{\text{argsort}(s)} = s^T$ since $P_{\text{argsort}(s)}^T P_{\text{argsort}(s)} = I$ (because $P_{\text{argsort}(s)}$ is a permutation matrix). Hence we arrive at:

$$\begin{aligned} &= \sigma\left(\frac{-d(\text{sort}(s)\mathbf{1}^T, \mathbf{1}s^T)}{\tau}\right) \\ &= \text{SoftSort}_\tau^d(s) \end{aligned}$$

which proves the proposition for SoftSort. ■

Proof of Proposition 1 for NeuralSort. For any fixed i , inspecting row i we get:

$$\begin{aligned} &(\text{NeuralSort}_\tau(\text{sort}(s)) P_{\text{argsort}(s)})[i, :] \\ &\stackrel{(i)}{=} (\text{NeuralSort}_\tau(\text{sort}(s))[i, :]) P_{\text{argsort}(s)} \\ &\stackrel{(ii)}{=} \sigma\left(\frac{(n+1-2i)\text{sort}(s)^T - \mathbf{1}^T A_{\text{sort}(s)}^T}{\tau}\right) P_{\text{argsort}(s)} \end{aligned}$$

where (i) follows since row-indexing and column permutation trivially commute, i.e. $(BP)[i, :] = (B[i, :])P$ for any $B \in \mathbb{R}^{n \times n}$, and (ii) is just the definition of NeuralSort (Eq. 3, taken as a row vector).

Using Lemma 2 we can push $P_{\text{argsort}(s)}$ into the softmax, and so we get:

$$\begin{aligned} &= \sigma\left(\left((n+1-2i)\text{sort}(s)^T P_{\text{argsort}(s)}\right. \right. \\ &\quad \left. \left. - \mathbf{1}^T A_{\text{sort}(s)}^T P_{\text{argsort}(s)}\right) / \tau\right) \end{aligned} \quad (13)$$

Now note that $\text{sort}(s)^T P_{\text{argsort}(s)} = s^T$ (as we showed in the proof of the Proposition for SoftSort). As for the subtracted term, we have, by definition of $A_{\text{sort}(s)}$:

$$\begin{aligned} &\mathbf{1}^T A_{\text{sort}(s)}^T P_{\text{argsort}(s)} \\ &= \mathbf{1}^T |\text{sort}(s)\mathbf{1}^T - \mathbf{1}\text{sort}(s)^T| P_{\text{argsort}(s)} \end{aligned}$$

Applying Lemma 1 to the pointwise absolute value, we can push $P_{\text{argsort}(s)}$ into the absolute value:

$$= \mathbf{1}^T |\text{sort}(s)\mathbf{1}^T P_{\text{argsort}(s)} - \mathbf{1}\text{sort}(s)^T P_{\text{argsort}(s)}|$$

Again we can simplify $\text{sort}(s)^T P_{\text{argsort}(s)} = s^T$ and $\mathbf{1}^T P_{\text{argsort}(s)} = \mathbf{1}^T$ to get:

$$= \mathbf{1}^T |\text{sort}(s)\mathbf{1}^T - \mathbf{1}s^T| \quad (14)$$

We are almost done. Now just note that we can replace $\text{sort}(s)$ in Eq. 14 by s because multiplication to the left by $\mathbf{1}^T$ adds up over each column of $|\text{sort}(s)\mathbf{1}^T - \mathbf{1}s^T|$ and thus makes the sort irrelevant, hence we get:

$$\begin{aligned} &= \mathbf{1}^T |s\mathbf{1}^T - \mathbf{1}s^T| \\ &= \mathbf{1}^T A_s \end{aligned}$$

Thus, putting both pieces together into Eq. 13 we arrive at:

$$\begin{aligned} &= \sigma\left(\frac{(n+1-2i)s - \mathbf{1}^T A_s}{\tau}\right) \\ &= \text{NeuralSort}_\tau(s)[i, :] \end{aligned}$$

which proves Proposition 1 for NeuralSort. ■

C. Proof of Proposition 2

First, let us recall the proposition:

Proposition. Let $k = 1$ and \hat{P} be the differentiable kNN operator using $\text{SoftSort}_2^{|\cdot|}$. If we choose the embedding function Φ to be of norm 1, then

$$\hat{P}(\hat{y}|\hat{x}, X, Y) = \sum_{i: y_i = \hat{y}} e^{\Phi(\hat{x}) \cdot \Phi(x_i)} / \sum_{i=1 \dots n} e^{\Phi(\hat{x}) \cdot \Phi(x_i)}$$

Proof. Since $k = 1$, only the first row of the SoftSort matrix is used in the result. Recall that the elements of the first row are the softmax over $-|s_i - s_{[1]}|$. Given that $s_{[1]} \geq s_i \forall i$, we can remove the negative absolute value terms. Because of the invariance of softmax for additive constants, the $s_{[1]}$ term can also be cancelled out.

Furthermore, since the embeddings are normalized, we have that $s_i = -\|\Phi(x_i) - \Phi(\hat{x})\|^2 = 2\Phi(x_i) \cdot \Phi(\hat{x}) - 2$. When we take the softmax with temperature 2, we are left with values proportional to $e^{\Phi(x_i) \cdot \Phi(\hat{x})}$. Finally, when the vector is multiplied by $\mathbb{1}_{Y=\hat{y}}$ we obtain the desired identity. ■

D. Magnitude of Matrix Entries

The outputs of the NeuralSort and SoftSort operators are $n \times n$ (unimodal) row-stochastic matrices, i.e. each of their rows add up to one. In section 4.1 we compared the mathematical complexity of equations 3 and 4 defining both operators, but how do these operators differ *numerically*? What can we say about the magnitude of the matrix entries?

For the $\text{SoftSort}^{|\cdot|}$ operator, we show that the values of a given row come from Laplace densities evaluated at the s_j . Concretely:

Proposition 3 For any $s \in \mathbb{R}^n$, $\tau > 0$ and $1 \leq i \leq n$, it holds that $\text{SoftSort}_\tau^{|\cdot|}(s)[i, j] \propto_j \phi_{\text{Laplace}(s_{[i]}, \tau)}(s_j)$. Here $\phi_{\text{Laplace}(\mu, b)}$ is the density of a Laplace distribution with location parameter $\mu \geq 0$ and scale parameter $b > 0$.

Proof. This is trivial, since:

$$\text{SoftSort}_\tau^{|\cdot|}(s)[i, j] = \frac{1}{\underbrace{\sum_{k=1}^n \exp\{-|s_{[i]} - s_k|/\tau\}}_{c_i}} \underbrace{\exp\{-|s_{[i]} - s_j|/\tau\}}_{\phi_{\text{Laplace}(s_{[i]}, \tau)}(s_j)}$$

where c_i a constant which does not depend on j (specifically, the normalizing constant for row i). □

In contrast, for the NeuralSort operator, we show that in the prototypical case when the values of s are equally spaced, the values of a given row of the NeuralSort operator come from *Gaussian* densities evaluated at the s_j . This is of course not true in general, but we believe that this case provides a meaningful insight into the NeuralSort operator. Without loss of generality, we will assume that the s_j are sorted in decreasing order (which we can, as argued in section 4.1); this conveniently simplifies the indexing. Our claim, concretely, is:

Proposition 4 Let $a, b \in \mathbb{R}$ with $a > 0$, and assume that $s_k = b - ak \forall k$. Let also $\tau > 0$ and $i \in \{1, 2, \dots, n\}$. Then $\text{NeuralSort}_\tau(s)[i, j] \propto_j \phi_{\mathcal{N}(s_i, a\tau)}(s_j)$. Here $\phi_{\mathcal{N}(\mu, \sigma^2)}$ is the density of a Gaussian distribution with mean $\mu \geq 0$ and variance $\sigma^2 > 0$.

Proof. The i, j -th logit of the NeuralSort operator before division by the temperature τ is (by Eq. 3):

$$\begin{aligned} &(n+1-2i)s_j - \sum_{k=1}^n |s_k - s_j| \\ &= (n+1-2i)(b-aj) - \sum_{k=1}^n |b-ak-b+aj| \\ &= (n+1-2i)(b-aj) - a \sum_{k=1}^n |j-k| \\ &= (n+1-2i)(b-aj) - a \frac{j(j-1)}{2} \\ &\quad - a \frac{(n-j)(n-j+1)}{2} \\ &= -a(i-j)^2 + a(i^2 - \frac{n^2}{2} - \frac{n}{2}) - b(2i-n-1) \\ &= -\frac{(s_i - s_j)^2}{a} + \underbrace{a(i^2 - \frac{n^2}{2} - \frac{n}{2}) - b(2i-n-1)}_{\Delta_i} \end{aligned}$$

where Δ_i is a constant that does not depend on j . Thus, after dividing by τ and taking softmax on the i -th row, Δ_i/τ vanishes and we are left with:

$$\text{NeuralSort}_\tau[i, j] = \frac{1}{\underbrace{\sum_{k=1}^n \exp\{-(s_i - s_k)^2/(a\tau)\}}_{c_i}} \underbrace{\exp\{-(s_i - s_j)^2/(a\tau)\}}_{\phi_{\mathcal{N}(s_i, a\tau)}(s_j)}$$

where c_i a constant which does not depend on j (specifically, the normalizing constant for row i). □

Gaussian densities can be obtained for SoftSort too by choosing $d = |\cdot|^2$. Indeed:

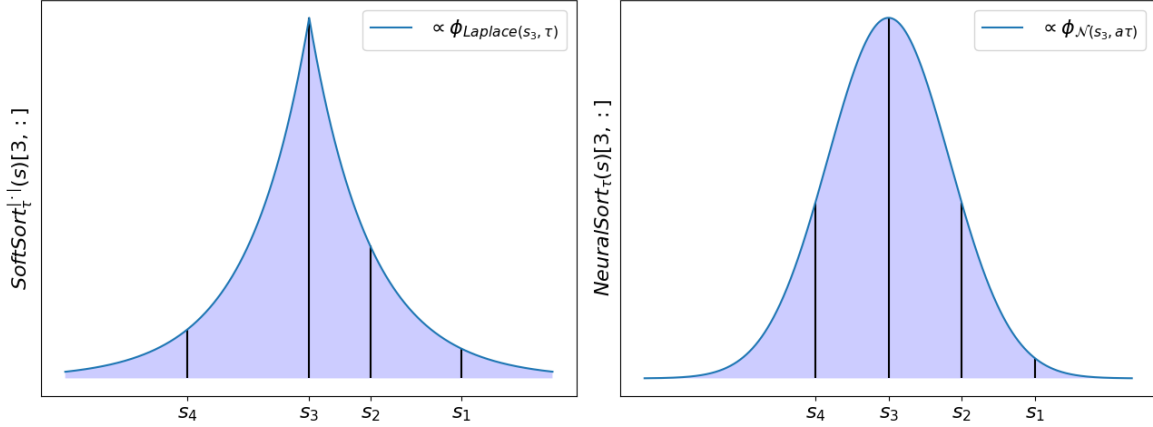


Figure 10. Rows of the $\text{SoftSort}^{|\cdot|}$ operator are proportional to Laplace densities evaluated at the s_j , while under the equal-spacing assumption, rows of the NeuralSort operator are proportional to Gaussian densities evaluated at the s_j . Similarly, rows of the $\text{SoftSort}^{|\cdot|^2}$ operator are proportional to Gaussian densities evaluated at the s_j (plot not shown).

Proposition 5 For any $s \in \mathbb{R}^n$, $\tau > 0$ and $1 \leq i \leq n$, it holds that $\text{SoftSort}_\tau^{|\cdot|^2}(s)[i, j] \propto_j \phi_{\mathcal{N}(s_{[i]}, \tau)}(s_j)$.

Proof. This is trivial, since:

$$\text{SoftSort}_\tau^{|\cdot|^2}(s)[i, j] = \frac{1}{\underbrace{\sum_{k=1}^n \exp\{-(s_{[i]} - s_k)^2 / \tau\}}_{c_i}} \underbrace{\exp\{-(s_{[i]} - s_j)^2 / \tau\}}_{\phi_{\mathcal{N}(s_{[i]}, \tau)}(s_j)}$$

where c_i a constant which does not depend on j (specifically, the normalizing constant for row i). \square

Figure 10 illustrates propositions 3 and 4. As far as we can tell, the Laplace-like and Gaussian-like nature of each operator is neither an advantage nor a disadvantage; as we show in the experimental section, both methods perform comparably on the benchmarks. Only on the speed comparison task does it seem like NeuralSort and $\text{SoftSort}^{|\cdot|^2}$ outperform $\text{SoftSort}^{|\cdot|}$.

Finally, we would like to remark that $\text{SoftSort}^{|\cdot|^2}$ does not recover the NeuralSort operator, not only because Proposition 4 only holds when the s_i are equally spaced, but also because even when they *are* equally spaced, the Gaussian in Proposition 4 has variance $a\tau$ whereas the Gaussian in Proposition 5 has variance τ . Concretely: we can only make the claim that $\text{SoftSort}_{a\tau}^{|\cdot|^2}(s) = \text{NeuralSort}_\tau(s)$ when s_i are equally spaced at distance a . As soon as the spacing between the s_i changes, we need to *change the temperature* of the $\text{SoftSort}^{|\cdot|^2}$ operator to match the NeuralSort operator again. Also, the fact that the $\text{SoftSort}^{|\cdot|^2}$ and NeuralSort operators agree in this prototypical case for some choice of τ does not mean

that their *gradients* agree. An interesting and under-explored avenue for future work might involve trying to understand how the *gradients* of the different continuous relaxations of the argsort operator proposed thus far compare, and whether some gradients are preferred over others. So far we only have empirical insights in terms of learning curves.

E. Sorting Task - Proportion of Individual Permutation Elements Correctly Identified

Table 5 shows the results for the second metric (the proportion of individual permutation elements correctly identified). Again, we report the mean and standard deviation over 10 runs. Note that this is a less stringent metric than the one reported in the main text. The results are analogous to those for the first metric, with SoftSort and NeuralSort performing identically for all n , and outperforming the method of (Cuturi et al., 2019) for $n = 9, 15$.

F. PyTorch Implementation

In Figure 12 we provide our PyTorch implementation for the $\text{SoftSort}^{|\cdot|}$ operator. Figure 11 shows the PyTorch implementation of the NeuralSort operator (Grover et al., 2019) for comparison, which is more complex.

Table 5. Results for the sorting task averaged over 10 runs. We report the mean and standard deviation for the *proportion of individual permutation elements correctly identified*.

ALGORITHM	$n = 3$	$n = 5$	$n = 7$	$n = 9$	$n = 15$
DETERMINISTIC NEURALSORT	0.946 ± 0.004	0.911 ± 0.005	0.882 ± 0.006	0.862 ± 0.006	0.802 ± 0.009
STOCHASTIC NEURALSORT	0.944 ± 0.004	0.912 ± 0.004	0.883 ± 0.005	0.860 ± 0.006	0.803 ± 0.009
DETERMINISTIC SOFTSORT	0.944 ± 0.004	0.910 ± 0.005	0.883 ± 0.007	0.861 ± 0.006	0.805 ± 0.007
STOCHASTIC SOFTSORT	0.944 ± 0.003	0.910 ± 0.002	0.884 ± 0.006	0.862 ± 0.008	0.802 ± 0.007
(CUTURI ET AL., 2019, REPORTED)	0.950	0.917	0.882	0.847	0.742

```
def neural_sort(s, tau):
    n = s.size()[1]
    one = torch.ones((n, 1), dtype = torch.float32)
    A_s = torch.abs(s - s.permute(0, 2, 1))
    B = torch.matmul(A_s, torch.matmul(one, torch.transpose(one, 0, 1)))
    scaling = (n + 1 - 2 * (torch.arange(n) + 1)).type(torch.float32)
    C = torch.matmul(s, scaling.unsqueeze(0))
    P_max = (C-B).permute(0, 2, 1)
    sm = torch.nn.Softmax(-1)
    P_hat = sm(P_max / tau)
    return P_hat
```

Figure 11. Implementation of NeuralSort in PyTorch as given in (Grover et al., 2019)

```
def soft_sort(s, tau):
    s_sorted = s.sort(descending=True, dim=1)[0]
    pairwise_distances = (s.transpose(1, 2) - s_sorted).abs().neg() / tau
    P_hat = pairwise_distances.softmax(-1)
    return P_hat
```

Figure 12. Implementation of SoftSort in PyTorch as proposed by us (with $d = |\cdot|$).